

# Numerical model of an industrial refrigeration system for condensation temperature optimisation

Michael Giovannini, Marco Lorenzini \*

University of Bologna, Department of Industrial Engineering, Via Fontanelle 40, I-47121, Forlì, Italy

## ARTICLE INFO

### Keywords:

Food refrigeration  
Energy consumption minimisation  
Evaporative condensers

## ABSTRACT

Refrigeration plants in the food industry have a key role, yet are very energy-intensive, which poses a serious problem given the current steep rise of energy prices. In this framework, energy consumption minimisation represents a paramount goal for plant managers, yet most are loathe to test new control strategies in real-life plants, lest normal operation be disrupted and food be spoiled as a consequence. In this view, numerical models able to demonstrate the reduction in energy consumption which can be achieved with suitable conduction strategies, especially in the case when evaporative condensers are employed, appear the ideal tool to provide the manager with an estimation of the potential savings and spur them into adopting such strategies. In this work one such model is developed for the primary loop of the refrigeration plant of a warehouse for food storage located in northern Italy. The choice of the model type is discussed at length, as are modelling issues related to all main components of the loop. The model has been validated with operational data from the real-life plant and employed to determine the optimal condensation pressure corresponding to the minimum total energy consumption according to ambient conditions. The method and model can be applied to other, similar plants in order to minimise their energy consumption.

## 1. Introduction

Vapour compression systems (VCSs) are widely employed in refrigeration plants serving warehouses and facilities for food storage. In spite of the relative simplicity of the base thermodynamic cycle, industrial applications can quickly become somewhat complex because of the presence of several auxiliary components and of the control logics needed to operate the whole plant. In the base cycle, the refrigerant operates at two different pressure levels, with compressor and expansion valve causing its pressure to change. In the common arrangements of industrial plants, the cooling loads are usually decoupled from the so called primary refrigeration loop, through the use of separator tanks, which collect the refrigerant at the lower pressure level, supplying dry vapour at the suction side of the compressor with modest degrees of superheating. In the primary refrigeration loop, the refrigerant is compressed from the low-pressure side to the high-pressure level, then after condensation the subcooled liquid is brought back to the low-pressure receiver through the expansion valves [1]. This configuration is also suitable to reduce the amount of refrigerant in the plant, especially for fluids which are highly toxic or have a significant global warming potential (GWP); another less problematic fluid can be used in the evaporator circuits, which interact with the primary refrigerant through heat exchangers. Concerning the overall management of the

plant, the system aims to keep the ideal temperature to ensure proper conservation of the stored goods, under all ambient conditions and with the lowest possible energy consumption. Due to the constraints imposed by correct food conservation, the main control variable available for optimisation of plant performance in terms of conduction costs is the condensation pressure, especially when evaporative condensers are employed [2], which, if correctly controlled, can improve VCSs performance significantly more than other single-fluid condensers, [3].

In this framework, mathematical modelling of the operation of the primary refrigeration loop allows evaluation of the change in condensation pressure as ambient conditions and cooling load vary, without the need to conduct complex and expensive experimental campaigns on an existing plant, which are often met with scepticism, when not open mistrust, by those owning and operating the plant. In the recent past, a few works have been presented which deal with the modelling of refrigeration plants, e.g. [4,5]. One of the key issues is the way in which system components are modelled. Three approaches can be identified, namely:

- Models based on operation maps, which are usually supplied by the manufacturers: they are very accurate within the operation

\* Corresponding author.

E-mail address: [marco.lorenzini@unibo.it](mailto:marco.lorenzini@unibo.it) (M. Lorenzini).

range mapped, but can have serious extrapolation errors when used outside that domain.

- Models based on physical principles: they allow a deeper understanding of the physical phenomena involved, granting a larger robustness to parameter variation. The drawback is the larger effort needed to define and validate them.
- Black-box models: they are obtained through a regression analysis, provided enough experimental data are available. The time for their development is usually shorter than for physical models, but they are prone to quickly lose in accuracy when used outside of the range of the experimental data used to define them.

One more issue to keep in mind is the definition of the time scale of interest, [5], and the choice between a steady-state or a time-dependent approach, depending on the model goals. If a control-oriented model is desired, a ‘quasi-steady’ approach can be chosen: in fact, if the dominant time scale of the inputs to the system has a different order of magnitude than that of the model, the dynamics of the latter can be described as a sequence of steady states, even if subject to time-varying conditions. Moreover, as highlighted by Bendapudi and Braun [5], the dominant time scale in a VCS depends on the heat transfer in the evaporators and condensers, considering that the compressors and expansion valves dynamic is faster by orders of magnitude than that of the heat transfer processes. Because of this, particular attention must be devoted to the thermal modelling of these components. On the other hand, given that the control logics for a VCS depends mainly on the pressures in the high- and low-pressure sections, which in large industrial plants are affected by the amount of refrigerant in the tanks, a control-oriented model suitable for plants of large size must be able to simulate mass variation in the storage elements whose dynamic behaviour becomes dominant in the system.

Finally, components can be modelled either with a distributed-parameter or a lumped-parameter approach. The latter is computationally less expensive, but is unable to describe the spatial variation of the physical phenomenon, and can only yield domain-averaged values for process variables. Conversely, the former approach allows a more detailed view of the process, which may be useful when defining control logics, but at the expenses of a larger computational effort.

The discussion above highlights the many issues which must be kept in mind when modelling refrigeration for control purposes, and can maybe explain why few works tackle the problem. This is also the aim of this work, which investigates an industrial refrigeration plant serving a food storage warehouse located in northern Italy. The ultimate goal is to demonstrate conduction strategies, i.e. how the plant should be operated in terms of condensation pressure, which minimise the total energy consumption of the plant. This was achieved through the definition of a mathematical model able to simulate the operation of a VCS under varying ambient conditions and cooling loads and numerically implementing it. The focus of this work is on the primary refrigeration loop, which includes the compression and condensation sections and the low- and high-pressure collector tanks, neglecting the detailed investigation of the secondary loop, which consists of all auxiliary circuits and of the evaporators operating in each food storage area within the warehouse: these are represented in the model by their cooling loads lumped into a single input. This choice is consistent with the main aim of the model, that is the determination of the set point for the condensation pressure minimising energy consumption for the plant under given ambient conditions and cooling loads. The model has been developed starting from the study of its main components and of their interaction, with particular attention to control issues which allow a correct set-point for operating pressures. The ‘quasi-steady’ approach has been adopted for the current model: the operation of compressors, condensers and expansion valves is simulated as a series of steady states following the change in inputs, treating the components as lumped-parameter models; only evaporative condensers have been modelled as distributed-parameter systems, owing to their key role in defining

**Table 1**  
Screw compressor characteristics.

	1	2	3
Power (kW)	160	200	315
Rotational speed (rpm)	3600	3600	3600
Capacity control valve	yes	yes	yes
Volume ratio control valve	yes	yes	yes
Inverter	no	yes	yes

**Table 2**  
Evaporative condensers characteristics and nominal operating points.

	1	2
Refrigerant	R717	R717
Fill pack	yes	no
Flow arrangement	co-flow	counter-flow
Maximum heat rejection (kW)	1783	1420
Condensation temperature (°C)	35	35
Air wet bulb temperature (°C)	26	25
Fan power (kW)	3 × 11	37
Air flow rate (m <sup>3</sup> s <sup>-1</sup> )	71.8	36.6
Pump power (kW)	7.5	5.5
Water flow rate (l s <sup>-1</sup> )	82.5	38.5

condensation pressure. The dynamic behaviour of the system has been entrusted to the high- and low-pressure collector tanks: in this way, the time evolution of the main control variables of the plant have been evaluated, namely the pressures and the amount of liquid refrigerant in the tanks. The mathematical model has been converted into a numerical model developed in Python, which is freely available, is comparatively easy to use and has a wide number of libraries available for a wide range of purposes.

## 2. Real-life plant

In this work an ammonia (R717) vapour compression cycle is analysed. The cycle is employed in a warehouse for food (vegetables and fruit) storage in northern Italy. A simplified sketch of the main refrigeration loop is shown in Fig. 1. The five screw compressors installed differ in cooling capacity and control mode available to each. Three types can be distinguished as summarised in Table 1. All compressors are equipped with slide valves which modulate the volumetric flowrate and independently adjust the volume ratio to the current inlet and outlet conditions so as to obtain maximum compressor efficiency. Further, three compressors are driven by motors equipped with inverters to vary the volumetric flowrate by continuously modifying the speed of revolution of the screws. In this configuration, the capacity control is carried out in two different ways: starting from the maximum allowable rotational speed, modulation is obtained by the inverter; when the speed is low enough, the slide valves come into action.

The high-pressure section of the loop consists of the collector tank for the liquid refrigerant and of four evaporative condensers of two different builds, as reported in Table 2. In one type of condenser the refrigerant flows inside a tube bundle which is sprinkled on the outside with water falling from above while a current of ambient air flows around it from below: the two cooling fluids are therefore in counterflow. In the other type of condenser, an element is introduced below the tube bundle which allows the evaporative heat transfer from the water dripping from the tubes and ambient air being sucked from below. In the latter realisation, water and air are thus in co-flow, Fig. 2.

In the low-pressure section several separator tanks which decouple the main refrigeration loop from the cooling loads corresponding to each storage cell. In order to build a model capable of determining the optimum set-point value for the condensation pressure it was decided to simplify this portion of the loop by grouping the four tanks into a single component, in which the total cooling load from all cells is also lumped together to yield a single value.

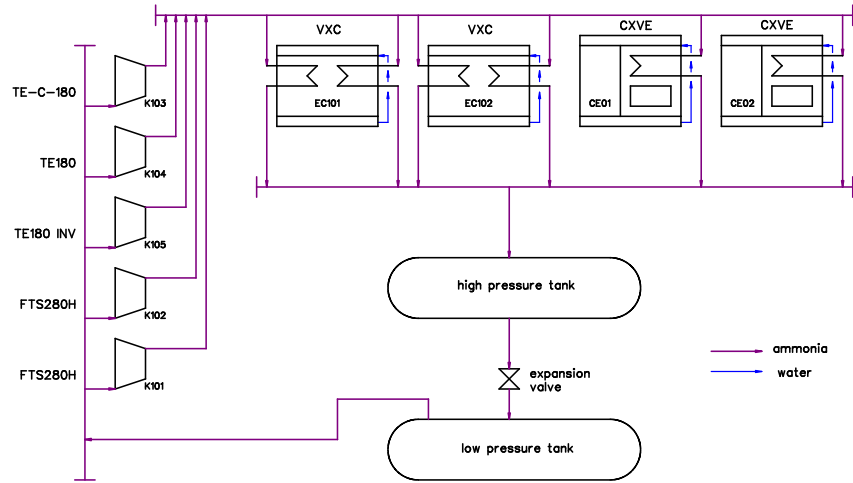


Fig. 1. Simplified scheme of the primary refrigeration loop of the plant.

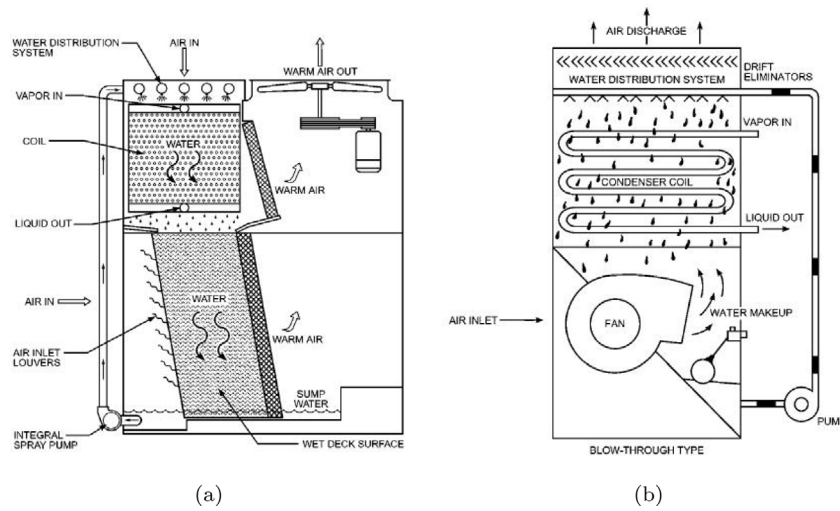


Fig. 2. Evaporative condenser schemes: (a) evaporative condenser with fill-pack in co-flow air-water arrangement along the coil and cross-flow air-water arrangement in the fill-pack; (b) evaporative condenser in counter-flow air-water arrangement, [6].

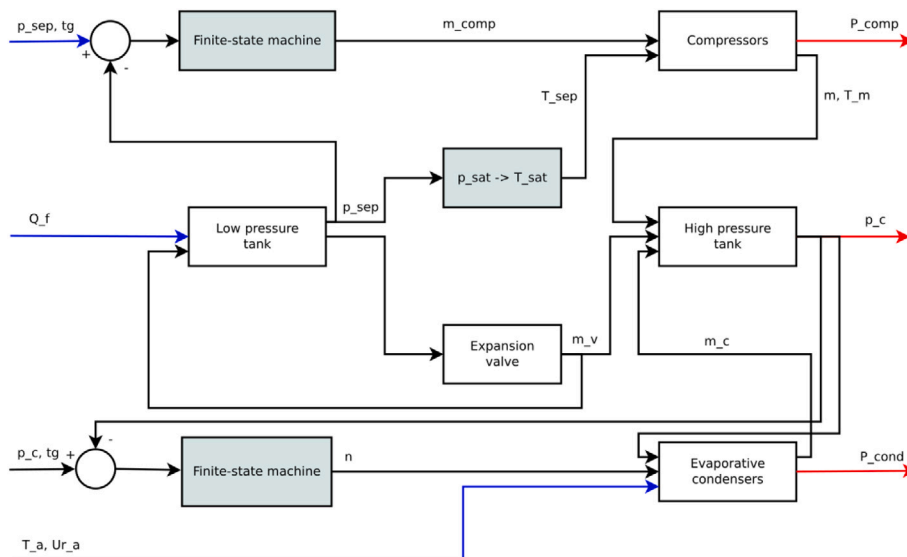


Fig. 3. Full primary refrigeration loop model block diagram.

### 3. Model structure

The mathematical model is sketched as a function block diagram in Fig. 3 and corresponds to the simplified layout of the actual cooling loop. Inputs to the model are ambient air conditions (temperature and relative humidity), the total cooling load required to keep the goods at the desired temperature and the set-points chosen for the condensation and evaporation pressure of the refrigeration cycle. The model outputs are the electric power required by the compressors, the thermal load dissipated by the evaporative condensers and the actual value of the condensation pressure, which can differ from the set-point owing to the influence of the actual ambient conditions on the heat transfer capability of the evaporative condensers and to the actual mass flowrate through the compressors. The main loop can be thought of as composed of two sections, which are defined by their operating pressures: the compression section and the condensation section. The former consists of the low-pressure tanks with their expansion valves, each modelled as one function block. The cooling load is supplied as an input to the low-pressure tank. In the same section, the five screw compressors can be considered as the actuators controlling the pressure level supplying the refrigerant mass flowrate needed to the high-pressure section. This is made up of four evaporative condensers and of the receiver. Again, the condensers can be seen as the actuators controlling the local pressure level by varying their heat transfer capability (and therewith the heat discharged to the ambient) through change in the speed of revolution of their fans. Thanks to this arrangement, the mass flowrate of condensed refrigerant is determined by the operating point of the condenser. The control logics underlying the model are summarised in Table 3 and are discussed further on.

Pressure drops along the piping and in the heat exchangers are not considered in this work, since the effects of changes in momentum transport are not decisive for simulations with comparatively large time steps, yet, this would not be allowable for short-term transient simulations, [7].

### 4. Function blocks of components

**Compressors.** Compressors have been described through a lumped-parameter model, since only input and output values of the main process variables need to be known. Compressor operation is therefore modelled using third-degree polynomials yielding electric energy consumption,  $P_e$ , refrigerant mass flowrate,  $\dot{m}$ , and temperature at the outlet,  $T_{out}$ , as a function of the independent variables, which are the saturation temperature at the compressor inlet and outlet. This method is in accordance with the international standards, such as EN 12900. The general process variable  $X = \{P_e, \dot{m}, T_{out}\}$  is computed through Eq. (1).

$$X = a_1 + a_2 T_e + a_3 T_c + a_4 T_e^2 + a_5 T_e T_c + a_6 T_c^2 + a_7 T_e^3 + a_8 T_e^2 T_c + a_9 T_e T_c^2 + a_{10} T_c^3 \quad (1)$$

Coefficients  $\bar{a} = \{a_1, \dots, a_{10}\}$  are a function of the speed of revolution of the compressor,  $n$ , and of the degree of superheat at the inlet,  $\Delta T_{sur,i}$ ,  $\bar{a} = f(n, \Delta T_{sur,i})$ ; they are usually supplied by the manufacturer. Since they were not available for some of the compressor installed, they have been obtained by processing data obtained during actual plant operation. Given the particular configuration of the primary refrigeration loop, the suction superheating is assumed constant; moreover, since the flow rate processed by the compressors depend both on the rotational speed and on the slide valve position,  $\bar{a} = f(\dot{m})$  is assumed. So, the actual mass flowrate range of each compressor is divided in twenty steps (5% of the whole range); the operating data are grouped into twenty bins; finally for each bin the coefficients  $\bar{a}$  of the polynomial correlations for the discharge temperature and for the power demand are determined by linear regression.

**Evaporative condensers.** The type of evaporative condensers differ for the relative direction of flow of the two cooling media, i.e. water and moist ambient air, and the possible presence of an additional piece of heat transfer equipment, called fill-pack, which allows a further cooling of the warmer water dripping from the tube bundle where condensation of the refrigerant occurs. Ambient air flows through the fill pack, usually in cross-flow with the water, and is then blown to the outside. Water cooled in the fill-pack is collected in a sump below it and pumped back to the sprinklers placed above the tube bundle of the condenser. The fill-pack enhances the cooling capability of the evaporative condenser thanks to the lower temperature of the water sprinkled over the tubes.

Several approaches to describe evaporative heat transfer, which is the way in which most thermal power is dissipated in this type of condensers, are described in the literature, [8–10], yet only a few are suitable for implementation in a model, as the one adopted in this study [11]. In this work the distributed-parameter description has been adopted which uses the theoretical description first proposed by Merkel, [12], and developed further by Dreyer, [13], and Kröger, [14].

The governing equations employed by the model of the tube bundle where condensation of the refrigerant occurs are listed below. The variation of air enthalpy through the tube bundle is calculated with:

$$dh_a = \frac{\beta}{\dot{m}_a} (h_{a,s} - h_a) dA_o \quad (2)$$

where the subscripts  $a$ ,  $s$  and  $o$  refer to air, saturation conditions and outer respectively, whereas  $\beta$  is the mass transfer coefficient,  $h$  is the specific enthalpy,  $A$  is the tube area. The refrigerant conditions along the tubes are estimated with:

$$dh_r = \frac{U}{\dot{m}_r} (T_r - T_w) dA_o \quad (3)$$

with  $U$  the overall heat transfer coefficient. In single phase condition, the refrigerant temperature can be calculated with:

$$dT_r = \frac{1}{c_{p,r}} dh_r \quad (4)$$

Finally the water temperature along the coils is computed as:

$$dT_w = \frac{1}{\dot{m} \cdot c_{p,w}} (\dot{m} dh_a + \dot{m}_r dh_r) \quad (5)$$

with  $w$  referring to water and  $r$  to refrigerant,  $T$  is the temperature and  $c_p$  the specific heat capacity at constant pressure. The equations yield moist air enthalpy, water temperature, refrigerant enthalpy and local temperature of the superheated refrigerant respectively.

The pressure drop for the refrigerant flowing within the cooling coil is considered negligible and all thermophysical and thermodynamic properties needed in the computations are obtained from data fits.

When the fill-pack is present, two more equations must be added, for air enthalpy and water temperature estimation:

$$dh_a = \frac{\beta_{fp}}{\dot{m}_a} (h_{a,s} - h_a) dA_o \quad (6)$$

$$dT_w = \frac{1}{\dot{m} \cdot c_{p,w}} \dot{m}_a dh_a \quad (7)$$

where the subscript  $fp$  refers to the fill-pack. Dreyer [13], obtained the relationship between the heat transfer area and the front area of the fill-pack  $A_{fr}$ , by the ratio of the interface area between water droplets and air to the volume of the fill-pack  $a_{fp}$ , so that for an element of length  $dz$ :

$$dA_{fp} = a_{fp} A_{fr} dz \quad (8)$$

Eqs. 2 to (4), together with Eqs. 6 to (8) when the fill-pack is present, constitute the core of the condenser blocks are numerically solved with a fixed-step Euler integration method, see [15] for the details, where an in-depth discussion of the issues related to the correct choice of the transport coefficients is also presented.

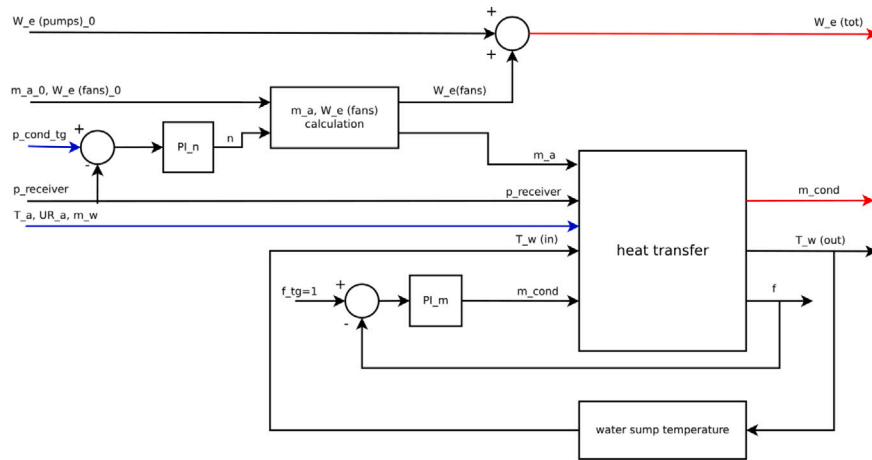


Fig. 4. Evaporative condensers function block.

In the counterflow condenser model an iterative loop is needed to estimate moist air conditions at the inlet to ensure that the computed values match the actual ones. Further, in both condenser models, a proportional-integral (PI) control forces the outlet mass flowrate of refrigerant to be either at saturated or slightly subcooled conditions: this is introduced to simulate the actual effect of the liquid trap downstream of the tube bundle, which imposes a liquid flow at the outlet. In both cases, another computational loop is used to let the water in the sump reach the steady-state temperature starting from ambient conditions. Finally, the speed of revolution of the fans is modulated so as to keep the desired condensation pressure; similar to the actual machine conduction, this is achieved by another PI controller which follows the imposed pressure set-point. The function block of the evaporative condenser is shown in Fig. 4.

**Tanks.** The low-pressure receivers of the plant are modelled as a single block, whose input is the cooling load derived from the activities in the warehouse and the need to keep the foodstuff at the desired storage temperature. The model is based on mass and energy balances, Eqs. (9) and (10) :

$$\frac{dM_t}{d\tau} = \dot{m}_v - \dot{m}_c \quad (9)$$

$$\frac{dE_t}{d\tau} = \dot{m}_v h_v - \dot{m}_c h_{vap} + \dot{Q}_f \quad (10)$$

where  $M$  is the total mass and  $E$  is the total internal energy of the refrigerant contained in the tank, as indicated by subscript  $t$ ; the subscripts  $v$  and  $c$  refer to expansion valve and compressor,  $vap$  refers to the saturated vapour condition of the refrigerant contained in the upper part of the tank. Finally  $\dot{Q}_f$  is the refrigeration load of the plant, which is represented as a lumped contribution occurring in the low pressure receiver.

The high-pressure receiver is also described by mass and energy balances, but the contribution of the cooling load is absent; moreover, some artificial connections between this receiver and the condensers have been introduced to simulate the actual behaviour of these components induced by the real pipeline configuration commonly used when evaporative condensers are involved [6]. Indeed, the mass flow rate from the compressor discharge feeds the high pressure collector, which supplies the refrigerant to the condensers; moreover, an equalisation pipeline connects this collector directly to the high-pressure receiver in order to guarantee that the condensate drains to the tank; for these reasons, neglecting the pressure drops, it is possible to assume that the receiver is at the same pressure as the condensers. This configuration is transposed in the model by assuming that the whole mass flowrate from the compressors goes to the high-pressure receiver. Then the condensers draw a certain amount of saturated vapour from the receiver and send it back as saturated liquid; the flow rate through the condensers depends on the heat transfer conditions.

**Table 3**  
Control logics for the function blocks.

Controlled variable	Actuator	Disturbance
Condensation pressure	Evaporative condensers	Discharge mass flow rate
Low pressure	Compressors	Inlet refrigerant mass flow rate Cooling load
Saturated liquid level	Expansion valve	Cooling load

**Expansion valve.** The expansion valves are located close to the corresponding low-pressure tanks and guarantee both the correct level of refrigerant in the tank and the desired pressure difference between the high-pressure section and the pressure within the tank itself. Since all tanks have been grouped into a single function block, the same has been done for the expansion valves. Similar to the actual operation of the valve, the refrigerant flow through the expansion valve is subject to a PI controller, to keep the liquid refrigerant within the low-pressure receiver at set-point value, as exemplified in Fig. 5.

## 5. Block connections

The components of the primary refrigeration loop described above must be connected to form a consistent model, able to simulate the actual operation of the plant. Again, this was achieved through implementation of suitable control strategies: Table 3 reports the way in which interaction between the function blocks is managed.

Compressors operate so as to follow the set-point pressure at the low-pressure collector at their inlet. The mass flowrate of R717 through the compressor is determined by its speed of revolution and by the position of its slide valve. The combined operation of all compressors is managed by a finite-state machine, which acts so that at any time only one compressor at most operates at partial load, whilst the others are either working at full load or switched off.

The amount of refrigerant in the low-pressure tank is defined by the expansion valve function block, in which a PI controller regulates the inlet flowrate from the high-pressure section to achieve the desired level of the liquid.

The high-pressure section, consisting of the four evaporative condensers and of the receiver tank, is controlled by setting the value for condensation pressure. Indeed, this quantity is dictated by the balance reached by the vapour and liquid phases of the refrigerant in the tank. While the amount of vapour increases thanks to the mass inflow from the compressors, the liquid inflow to the high-pressure receiver is determined by the heat transfer in the evaporative condensers. Because of this, control of the condensation pressure occurs through changes in the heat transfer capability of the condensers, which depends on the air

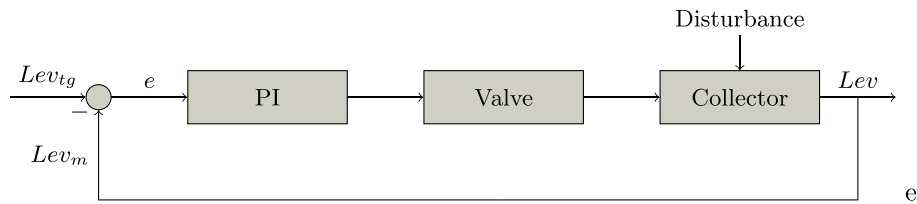


Fig. 5. Block scheme of the expansion valve.  $Lev$  refers to the saturated liquid level in the tank, the subscripts  $tg$  states for target, while  $m$  for measured;  $e$  is the error between the measured level and the target value.

Table 4  
Range for inputs and outputs used for validation phase.

	max	min
Input values		
Refrigeration load (kW)	1620.5	561.3
Temperature in low pressure receivers (°C)	-7.9	-11.7
Condensation temperature (°C)	27.4	22.9
Ambient wet bulb temperature (°C)	24.3	17.6
Calculated outputs		
Total power demand (kW)	516.4	216.41
Compressors power demand (kW)	414.3	128.4
Condensers power demand (kW)	172.0	58.4
Heat rejection at the condensers (kW)	1467.4	494.8

flowrate through their fans, determined by their rotational speed. The model of the primary refrigeration loop must be able to compute the actual pressure achieved during condensation depending on the ambient conditions, on the refrigerant flowrate from the compressors and on the speed of revolution of the fans. As mentioned before uniform pressure is assumed throughout the whole section, so that conditions in the tank dictate the condensation pressure. Control of condensation pressure is obtained through another PI logic, acting on fan speed. Furthermore, simultaneous operation of the evaporative condensers is managed, as for the compressors, through a finite-state machine allowing a single condenser at most to operate at partial load, while all the others are either inactive or running at full load. Although this mode of operation does not correspond to the actual strategy most often employed by plant technicians, the analysis of this comparatively simple technique can be taken as a starting point to evaluate other, more complex activation sequences, which might also be fully automated.

## 6. Results and discussion

The mathematical model has been translated into a computational model using the Python programming language. The code developed is able to simulate the behaviour of the whole loop when subjected to time variations of the input quantities as a succession of steady-state computations in the single function blocks, i.e. through a 'quasi-steady' approach. Only the dynamics of the mass accumulation in the tanks are taken into account to develop a model suitable for pressure control design of a large refrigeration plant.

### 6.1. Validation

Model validation was carried out comparing the behaviour of the actual primary refrigeration loop during steady-state operations with the results of the model under the same operating conditions. The model was run with different sets of inputs (ambient air temperature and relative humidity, evaporation and condensation pressures and total refrigeration load), each set representing a steady-state operation point; for each set, the outputs obtained and compared to real-life values are the power consumption of the compressors and of the evaporative condensers (to power their fans) and the thermal power dissipated through condensation. Data were collected during normal operation of

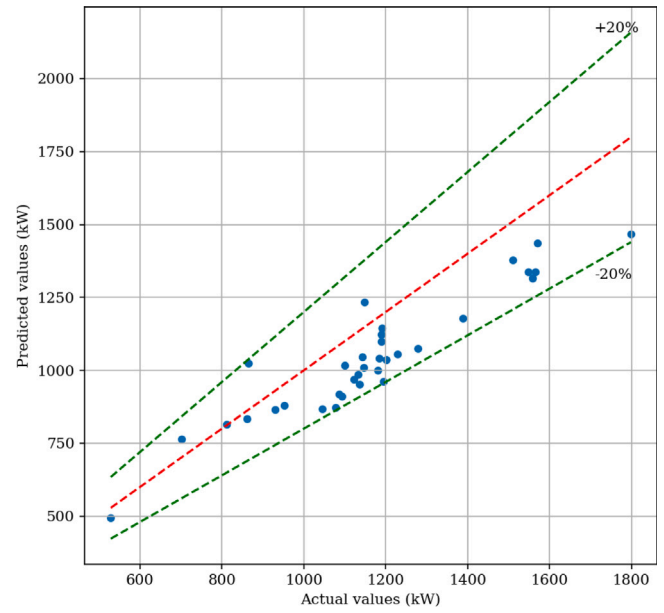


Fig. 6. Heat rejection at the condensers (kW).

the plant in August 2020. In order for the results to be comparable with the actual data from the plant, operating points were deemed stationary when condensation pressure would not oscillate more than  $\pm 1\%$  from its average value over a time span of at least 15 min. In Table 4, inputs (measured data) and calculated outputs of the model are summarised with their maximum and minimum values for the timespan considered.

The results are shown in Figs. 6 to 8 that plots the actual data against the ones calculated for the heat rejection at the condensers, for the compressors power demand and for the total power demand of the plant, respectively; it can be appreciated how the model, in spite of its comparative simplicity, is able to replicate the actual data (whose measurements are themselves affected by uncertainties) to within  $\pm 20\%$ . Results concerning total power demand, Fig. 8, are mostly within  $\pm 15\%$  of the measured values.

### 6.2. Condensation pressure control

The model can also be employed to predict the best condensation pressure set-point as a function of ambient temperature and relative humidity to minimise the total power consumption of the plant. This is of particular relevance for evaporative condensers, which allow condensation at a temperature close to that of wet bulb for the ambient air, but which are usually run at much larger values, especially when food storage is concerned; indeed, the technicians implements safe actions of control to avoid any risk of the goods being spoilt. The model can be used to demonstrate how the cooling load under given ambient conditions can be completely satisfied and what the savings in power

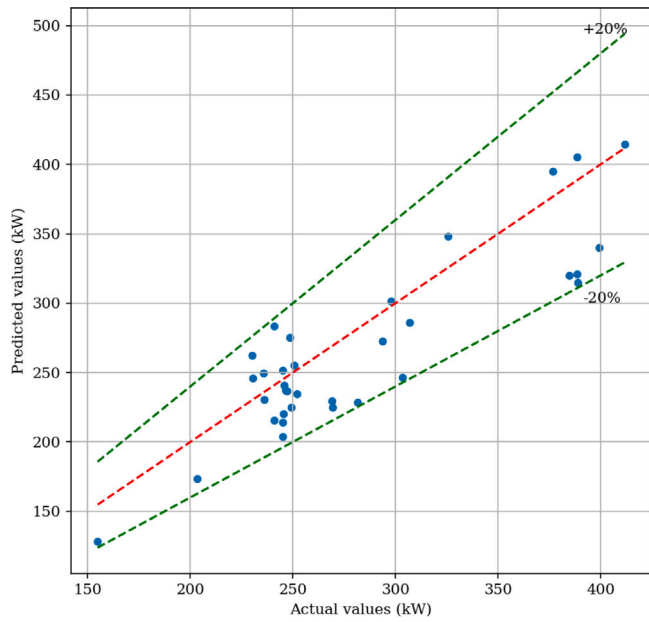


Fig. 7. Power demand by the compressors (kW).

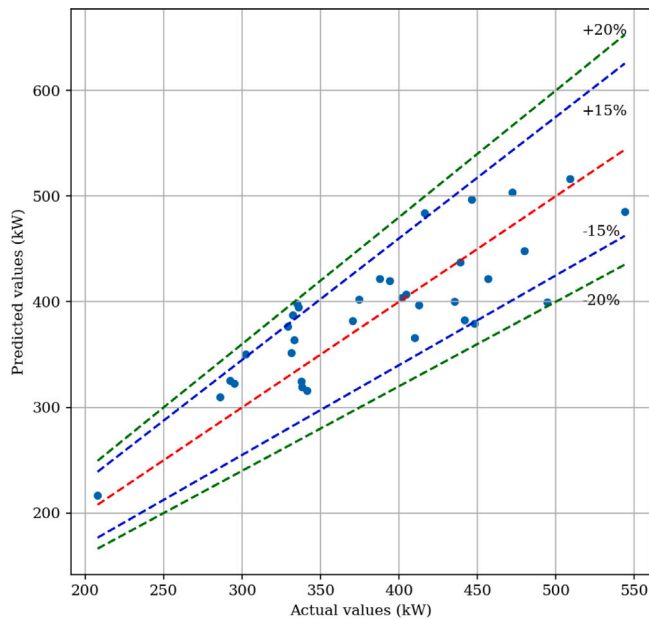


Fig. 8. Total power demand (kW).

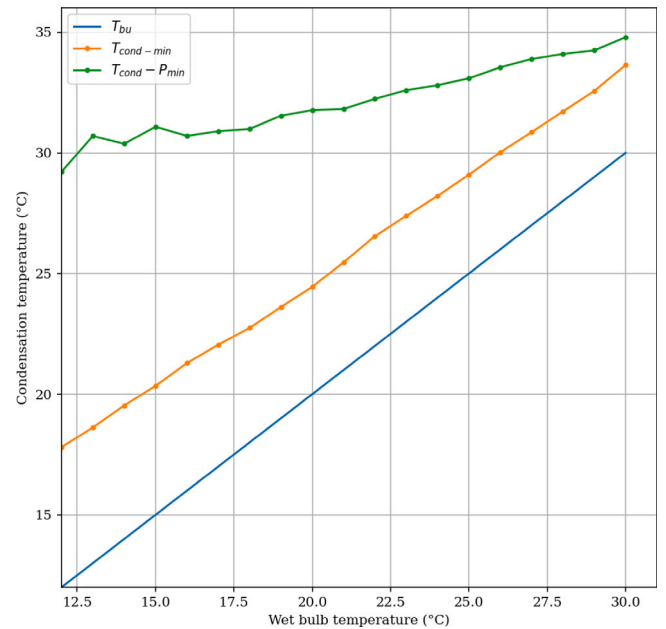


Fig. 9. Condensation temperature minimising electrical energy consumption (green) for a given wet bulb temperature. Minimum achievable condensation temperature (orange) for a given wet bulb temperature. Wet bulb temperature (blue).

consumption are in comparison to a more conservative operation mode, which uses high set-points for the condensation temperature.

To this aim, a set of simulations has been carried out to explore the predicted behaviour of the system by varying outdoor wet bulb temperature and condensation temperature; the refrigeration load and the low saturation pressure were assumed constant. In Table 5 the inputs and the outputs of the model are summarised with the corresponding ranges involved in these simulations. Fig. 9 shows the condensation temperature which minimises the total power consumption (i.e. of the compressors and fans) as a function of the wet bulb temperature of the ambient air, for a fixed value of refrigeration load equal to 1000 kW. The minimum possible condensation temperature as a function of wet bulb temperature is also shown for the same range of conditions; this temperature depends on the characteristics and on the sizing of the evaporative condensers. It can be seen easily that the optimum condensation pressure is invariably higher than the minimum allowable value for the same conditions: this can be explained remembering that fan operation is also required, and the minimum energy consumption must strike a balance between the savings in operating the compressors at lower condensation temperatures and the increase in power consumption of the fans under the same conditions.

7. Conclusions

In this work the model of a primary refrigeration loop used in a food storage facility has been developed. The components of the plant were described as function blocks, through which the time-dependent behaviour of the system was simulated using a ‘quasi-steady’ approach, which only accounts for the refrigerant accumulation dynamics which are most significant in term of system control. Components were modelled following a lumped-parameter approach, with the exception of the evaporative condensers, for which a distributed-parameter description was deemed more suitable. This choice was dictated by the need of an accurate estimate of the heat and mass transfer in these components, which are crucial for the determination of the condensation pressure in the refrigeration loop. Indeed, this approach allows mapping of the enthalpy for both moist air and liquid water over the whole extension of the cooling coil and, when present, of the fill-pack, and of the

Table 5  
Range for inputs and outputs used for optimisation phase.

	max	min
Input values		
Refrigeration load (kW)	1000.0	1000.0
Temperature in low pressure receivers (°C)	-10.0	-10.0
Condensation temperature (°C)	35.0	18.0
Ambient wet bulb temperature (°C)	30.0	0.0
Calculated outputs		
Total power demand (kW)	844.0	220.1
Compressors power demand (kW)	672.0	209.0
Condensers power demand (kW)	172.0	0.7
Heat rejection at the condensers (kW)	973.6	719.2

refrigerant condensation temperature and mass distribution within the tubes, as detailed in [16]. The model was validated against data collected during operation of the real-life plant. Simulations yield results falling within  $\pm 20\%$  of the experimental values for the condensation load and are even more accurate for the energy consumption of the compressors. Finally, a strategy has been developed to obtain the condensation pressure set-point causing the minimum total energy consumption (compressors and fans) for given ambient conditions, in particular the wet bulb temperature of ambient air. The method presented and the model developed are of general validity, and can be applied to other food storage facilities operating with the same type of equipment, and this feature gives the work a broad significance.

#### Declaration of competing interest

The authors declare that they have no known competing financial interests or personal relationships that could have appeared to influence the work reported in this paper.

#### Data availability

Data will be made available on request

#### References

- [1] American Society of Refrigeration Heating Air-Conditioning Engineers, 2018 ASHRAE Handbook: Refrigeration, ASHRAE, URL <https://books.google.it/books?id=-R7GwwEACAAJ>.
- [2] K. Manske, D. Reindl, S. Klein, Evaporative condenser control in industrial refrigeration systems, *Int. J. Refrig.* 24 (7) (2001) 676–691.
- [3] K. Harby, D.R. Gebaly, N.S. Koura, M.S. Hassan, Performance improvement of vapor compression cooling systems using evaporative condenser: an overview, *Renew. Sustain. Energy Rev.* 58 (2016) 347–360, <http://dx.doi.org/10.1016/j.rser.2015.12.313>.
- [4] B.P. Rasmussen, Dynamic modeling for vapor compression systems—Part I: Literature review, *HVAC&R Res.* 18 (5) (2012) 934–955.
- [5] S. Bendapudi, J.E. Braun, A Review of Literature on Dynamic Models of Vapor Compression Equipment, Tech. rep., ASHRAE, 2002.
- [6] American Society of Refrigeration Heating Air-Conditioning Engineers, Ashrae Handbook 2016: HVAC Systems and Equipment: SI Edition, in: ASHRAE Handbook of Heating, Ventilating and Air-Conditioning Systems and Equipment SI, ASHRAE, 2016, URL <https://books.google.it/books?id=iwCJAQAACAAJ>.
- [7] W.-J. Zhang, C.-L. Zhang, G.-L. Ding, On three forms of momentum equation in transient modeling of residential refrigeration systems, *Int. J. Refrig.* 32 (5) (2009) 938–944, <http://dx.doi.org/10.1016/j.ijrefrig.2008.11.002>.
- [8] J. Facao, A.C. Oliveira, Heat and Mass Transfer in an Indirect Contact Cooling Tower: CFD Simulation and Experiment, Vol. 54, Publisher: Taylor & Francis, pp. 933–944, (10).
- [9] A. Hasan, K. Sirén, Theoretical and computational analysis of closed wet cooling towers and its applications in cooling of buildings, 34 (5) 477–486. [http://dx.doi.org/10.1016/S0378-7788\(01\)00131-1](http://dx.doi.org/10.1016/S0378-7788(01)00131-1) URL <https://www.sciencedirect.com/science/article/pii/S0378778801001311>.
- [10] W. Zalewski, Mathematical model of heat and mass transfer processes in evaporative condensers, 16 (1) 23–30. [http://dx.doi.org/10.1016/0140-7007\(93\)90017-3](http://dx.doi.org/10.1016/0140-7007(93)90017-3) URL <https://www.sciencedirect.com/science/article/pii/0140700793900173>.
- [11] P. Li, H. Qiao, Y. Li, J.E. Seem, J. Winkler, X. Li, Recent advances in dynamic modeling of HVAC equipment. Part 1: Equipment modeling, *HVAC&R Res.* 20 (1) (2014) 136–149.
- [12] F. Merkel, no. 275, Verdunstungskühlung, Vol. 70, VDI Forschungsarbeiten, Berlin, Germany, 1925, pp. 123–128.
- [13] A.A. Dreyer, Analysis of Evaporative Coolers and Condensers (Ph.D. thesis), Stellenbosch University, Stellenbosch, 1988.
- [14] D.G. Kröger, Air-Cooled Heat Exchangers and Cooling Towers, Vol. 1, PennWell Books, 2004.
- [15] M. Giovannini, M. Lorenzini, Sensitivity analysis to heat transfer correlation of the model for an evaporative condenser, in: ATE-HEFAT Virtual Conference 2021, Amsterdam (Online), 2021, pp. 1961–1966.
- [16] M. Giovannini, M. Lorenzini, Numerical model of an evaporative condenser for the food refrigeration industry, *J. Phys. Conf. Ser.* 2177 (1) (2022) 012009, <http://dx.doi.org/10.1088/1742-6596/2177/1/012009>.